

Trimetazidine attenuates dexamethasone-induced muscle atrophy via inhibiting NLRP3/GSDMD pathway-mediated pyroptosis

Li Wang ^{a,b,†}, Ming-Qing He ^{c,†}, Xi-Yu Shen ^{a,b}, Kang-Zhen Zhang ^{a,b}, Can Zhao ^{a,b}, Li Liu ^{a,b}, Man Wang ^{a,b}, Yun-Ling Bu ^{a,b}, Jia-Wen Li ^{a,b}, Fan Xu ^{a,b}, Hui-Wei He ^{a,b}, Xiang Lu ^{a,b,*}, Wei Gao ^{a,b,*}

^a Department of Geriatrics, Sir Run Run Hospital, Nanjing Medical University, China

^b Key Laboratory for Aging & Disease, Nanjing Medical University, Nanjing, China

^c Department of Geriatrics, The First Affiliated Hospital of Soochow University, Soochow University, Suzhou, China.

[†] These authors contributed equally to this work

*** Corresponding author:** Wei Gao, MD, PhD, Department of Geriatrics, Sir Run Run Hospital, Nanjing Medical University, 109 Longmian Avenue, Nanjing, 211166, Jiangsu Province, China. E-mail:gaowei84@njmu.edu.cn, Tel./Fax:0086-25-87115509; Xiang Lu, MD, PhD, Department of Geriatrics, Sir Run Run Hospital, Nanjing Medical University, 109 Longmian Avenue, Nanjing, 211166, Jiangsu Province China. E-mail: luxiang66@njmu.edu.cn, Tel./Fax: 0086-25-87115509.

Abstract

Skeletal muscle atrophy is one of the major side effects of high dose or sustained usage of glucocorticoids. Pyroptosis is a novel form of pro-inflammatory programmed cell death that may contribute to skeletal muscle injury. Trimetazidine, a well-known anti-anginal agent, can also improve skeletal muscle performance both in human and mice. We here showed that dexamethasone induced atrophy, evidenced by the increase of muscle atrophy F-box (Atrogin-1) and muscle ring finger 1 (MuRF1) expression, and the decrease of myotube diameter in C2C12 myotubes. Dexamethasone also induced pyroptosis, indicated by upregulated pyroptosis-related protein NLRP3, Caspase-1 and GSDMD. Knockdown of NLRP3 or GSDMD attenuated dexamethasone-induced myotube pyroptosis and atrophy. Trimetazidine administration ameliorated dexamethasone-induced muscle atrophy both *in vivo* and *in vitro*. Moreover, trimetazidine improved exercise tolerance, as evidenced by increased running distance and running time, as well as increased skeletal muscle mass in dexamethasone-treated mice. Mechanically, trimetazidine could reverse dexamethasone-induced activation of pyroptosis both in C2C12 myotubes and in mice. Taken together, our present study demonstrated that NLRP3/GSDMD pathway-mediated pyroptosis was involved in dexamethasone-induced skeletal muscle atrophy. Trimetazidine could partially alleviate dexamethasone-induced skeletal muscle atrophy, and increase the diameter of C2C12 myotubes via inhibiting pyroptosis. Thus, trimetazidine might be a potential therapeutic compound for the prevention of muscle atrophy in glucocorticoid-treated patients.

Keywords Dexamethasone; Muscle atrophy; Pyroptosis; Trimetazidine

Introduction

The loss of muscle mass and strength or physical function (sarcopenia) is one of the common disabilities in the elderly [1]. Muscle atrophy usually causes impairment of physical function, such as slowing of movement and muscle weakness, which is associated with increased morbidity and mortality [2]. It occurs under various conditions, such as aging [3], cancer [4], malnutrition [5], cardiac failure [6], obesity [7], as well as drug treatment [8]. Glucocorticoids are known to have catabolic effects on skeletal muscle, either as an endogenous endocrine hormone released in response to various stressful conditions or as a drug given exogenously to treat inflammation [9]. However, the sustained elevated levels of glucocorticoids result in a decrease in protein synthesis and an increase in proteolysis in skeletal muscle, ultimately leading to muscle atrophy and frailty [10]. Although several growth factors have been indicated that may play important roles in mediating glucocorticoids' effects on muscle mass and function [11], the exact underlying molecular mechanisms remain unclear and the effective treatment for glucocorticoids-induced muscle atrophy needs to be further elucidated.

Despite the extensive use of glucocorticoids as anti-inflammatory agents, emerging evidence indicates that glucocorticoids can also activate inflammatory signaling pathways as mechanism of inducing muscle atrophy [12]. Pyroptosis is a novel pro-inflammatory programmed cell death, which is characterized by cleavage of the pore-forming protein gasdermin-D (GSDMD) and formation of cytotoxic pores in the plasma membrane [13]. To date, the best characterized upstream activators of pyroptosis are inflammasome-signaling pathway components, such as nucleotide oligomerization domain (NOD)-like receptors (NLRs) [14]. Activation of NLRP3 inflammasome trigger Caspase-1 dependent pyroptosis accompanied with the release of inflammatory factors, such as interleukin (IL)-1 β and IL-18 [14]. Recent studies have demonstrated that pyroptosis plays an important role in the progression of muscle atrophy [15]. However, the mechanisms to which pyroptosis may contribute to the atrophy of skeletal muscle induces by dexamethasone is currently unclear.

Trimetazidine has been used as anti-anginal agent for decades. Trimetazidine exerts cardioprotective effects by shifting energy production from fatty acid oxidation to glucose oxidation [16]. Besides its cardiac protection ability, recent evidence suggests that trimetazidine can also improve skeletal muscle performance both in human and mice [17, 18]. Molinari F *et al.* [19] showed that trimetazidine could act like an 'exercise mimetic' in cancer cachexia through activating pathways known to increase protein synthesis and to reduce protein degradation. Another study found that trimetazidine protected muscle cells against starvation or inflammation-induced atrophy by inhibiting protein degradation and inducing autophagy [20]. In statin-induced skeletal muscle injury model, trimetazidine could alleviate simvastatin-induced exercise intolerance and muscle damages by ameliorating energy metabolism dysfunction and facilitating fast-to-slow type shift [21]. However, studies examining the benefits of trimetazidine in glucocorticoids-induced skeletal muscle atrophy are limited. Interestingly, trimetazidine has recently been shown to ameliorate lipopolysaccharide-induced cardiomyocyte pyroptosis by promoting neutrophil migration to cardiac tissue [22]. In the present study, we sought to explore the role and underlying mechanism of trimetazidine in the regulation of pyroptosis in a dexamethasone-induced muscle atrophy model.

Materials and methods

C2C12 myoblasts culture and differentiation

Murine C2C12 myoblasts were obtained from ATCC and incubated at 37 °C, 5% CO₂ in DMEM (Key GEN BioTECH, China) with 80U/ml penicillin and 0.08mg/ml streptomycin and 10% fetal bovine serum (Gibco). C2C12 myoblasts were within 10 generations. For induction of differentiation into myotubes, sub-confluent myoblasts were switched to DMEM containing 2% inactivated horse serum (Biological Industries, Israel), and then cultured for 4 days. The medium was changed every other day. All cell experiments were performed on C2C12 mature myotubes. The myotubes were treated with 10μM dexamethasone for 24 hours, and 150μM trimetazidine was added in the last 6 hours.

Cell viability

Cell viability was evaluated using CCK-8 assays (Dojindo, Japan). C2C12 cells were seeded in 96-well plates at a density of 1×10^4 cells per well. After fully differentiated, myotubes were treated with incremental dosages of dexamethasone (0.1, 1, 10μM) for 24 hours, and different concentrations of trimetazidine (50, 100, 150, 200μM) were added in the last 6 hours. CCK-8 reagent was added to each well and the absorbance was measured at 450 nm after 2 hours incubation by a microplate reader (Synergy H1, BioTek, US). The calculation equation for relative cell viability was as follows: cell viability (%) = (As - Ab) / (Ac - Ab) × 100%. As, Ab, and Ac were the absorptions of test sample, background, and control (DMSO), respectively.

Small interfering RNA (siRNA)

Chemically synthesized double-stranded siRNA duplexes targeting mouse NLRP3 (No. siG1161091244) and GSDMD (No. siG180420040947) were obtained from RiboBio Co., Ltd. (Guangzhou, China). For silencing NLRP3 or GSDMD, C2C12 myotubes were transfected with siRNA at day-4 post-differentiation by using RNAiMAX (Invitrogen, US) for 24 hours following treatment with dexamethasone.

Mice

C57BL/6J male mice of 8 weeks old were housed at a controlled temperature of 24±2°C and a relative humidity of 45±15% with a 12h light/dark cycle. Mice had free access to food and water. Mice were randomized into four groups (n=8) and intraperitoneally injected accordingly for 10 days: control (0.9% saline), dexamethasone (25mg/kg) (Catalog No. D4902, Sigma), trimetazidine (5 mg/kg) (Catalog No. 653322, Sigma), dexamethasone (25 mg/kg) +trimetazidine (5 mg/kg). All of the animal experiments were carried out under the approval of the Animal Ethics Committee of Nanjing University and complied with the National Institutes of Health guide for the care and use of Laboratory animals (NIH Publications No. 8023, revised 1978)

Running test

Exercise tolerance test was performed at the end of experiment using a mouse treadmill (Zhishuduobao DB030, China). The running protocol referred to previously published articles²¹ and combined actual conditions. The running speed was started at 8 m/min and increased 2 m/minute every 4 minutes. The slope of track was started at 0°, increased 1° every 4 minutes, and maintained at 14° because of limit of the treadmill. Adaptation training (8 m/minute, 0°, 2 minutes) was provided before the assessment of running tolerance. The time and distance were recorded when the mice were exhausted. The criterion for exhaustion was defined as touching electric grid for more than 5 seconds [23].

Protein extraction and Western blot analysis

Myotubes or gastrocnemius samples were lysed with cold RIPA buffer (Beyotime Biotechnology, Shanghai, China) containing 1 mM NaF, 1 mM sodium orthovanadate,

and 1 mM phenylmethylsulfonyl fluoride. Protein concentration was quantified using a BCA protein assay kit (Beyotime Biotechnology, Shanghai, China). Equal amount of protein was separated by 4-20% SDS-PAGE (GenScript Biotechnology, Nanjing, China), transferred to PVDF membranes (Millipore, Billerica, MA, USA), and then blocked with 5% nonfat milk in TBST buffer for 2 hours at room temperature. Membranes were incubated with specific primary antibody overnight at 4°C. The horseradish peroxidase conjugated secondary antibody was incubated for 1.5 hours at room temperature, then the immune complexes were detected by Immobilon Western HRP Substrate Peroxide Solution (Millipore Corporation, Billerica, MA 01821, USA). Images were acquired using ChemiDoc™ XRS+ Imaging System (Bio-Rad, USA). Band densitometry measurements were assessed using Image Lab 6.0 software. All the primary antibodies were listed in Table S1.

Isolation of total RNA and Real-time PCR analysis

Total RNA from C2C12 myotubes samples was isolated by RNA simple Total RNA Extraction Kit (dp419, TIANGEN, China) following the manufacturer's instructions. cDNA was synthesized using PrimeScript™ RT reagent Kit (Perfect Real Time) (RR047A, Takara, Japan). Quantitative Real-time PCR was performed using Maxima SYBR Green/ROX qPCR Master Mix (2X) (Thermo Scientific, K0221, USA) on QuantStudio 5 system (Applied Biosystems, USA). The relative gene expression levels were calculated by the $2^{-\Delta\Delta C_t}$ method using Glyceraldehyde 3-phosphate dehydrogenase (GAPDH) as an internal control. All the primer sequences were listed in Table S2.

Immunofluorescence and myotube diameter measurement

C2C12 cells were fixed with 4% paraformaldehyde for 20 minutes, permeabilized with 0.5% Triton X-100 in PBS for 15 minutes, and then blocked with 5% BSA in PBST for 1 hour at room temperature. Cells were incubated with anti-MHC (1:200, MF20, DSHB) overnight at 4°C. Cells were washed three times and incubated with secondary antibody Cy3-AffiniPure Rabbit Anti-Mouse IgG (H+L) (1:500, Jackson) for 1 hour at room temperature. Nuclear counterstaining was performed with DAPI. Images were captured using fluorescence microscope (Zeiss Axio Scope, Germany). Myotube diameter analysis was performed as previously published [24]. Briefly, ten fields were chosen randomly, and ten myotubes were measured per field by ImageJ (National Institutes of Health, USA). The average diameter per myotube was calculated as the mean of ten measurements taken along the long axis of the myotube.

Haematoxylin-eosin (HE) staining

Fresh gastrocnemius samples were fixed with 4% paraformaldehyde overnight, and embedded with paraffin, serially sliced to 4 µm for HE staining, following the standard staining procedures. For muscle fiber cross-sectional area analysis, images were captured using microscope (Zeiss Axio Scope.A1, Germany). As previously published [25], the diameter of myofiber was calculated by using the ImageJ software (National Institutes of Health, USA) in five random fields of each section.

Statistical analysis

Data were presented as mean ± SEM and analyzed by SPSS 21.0. One-way analysis of variance (ANOVA) followed by a Least Significant Difference test was used to compare conditions in myotubes and animal experiments. Significance was accepted as $P < 0.05$.

Results

Pyroptosis is activated in dexamethasone-induced C2C12 myotube atrophy

Inflammation plays a crucial role in the development of muscle atrophy [15], we first

determined whether pyroptosis was activated in dexamethasone-induced myotube atrophy. To form mature myotubes, C2C12 myoblasts were incubated with differentiation medium for 4 days until cell fusion (Figure S1). Dexamethasone at concentrations of 0.1 μ M and 1 μ M did not affect cell viability of C2C12 myotubes, while 10 μ M dexamethasone induced cell death (Figure 1A). Moreover, 10 μ M dexamethasone significantly increased the mRNA levels of Atrogin-1 and MuRF1 in C2C12 myotubes (Figure 1B). Similar results were observed in the protein levels of Atrogin-1 and MuRF1 at the dose of 10 μ M (Figure 1C). Importantly, the protein levels of pyroptosis-related molecules, including NLRP3, Caspase-1 and GSDMD were elevated in dexamethasone-treated C2C12 myotubes (Figure 1D), indicating that pyroptosis was activated in dexamethasone-induced myotube atrophy.

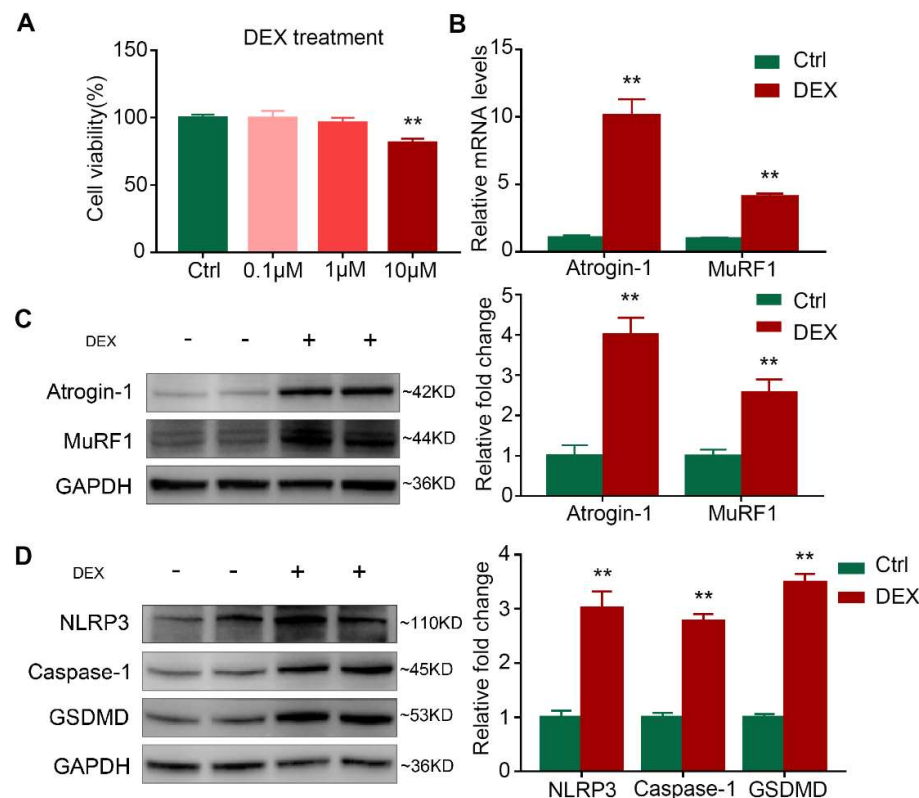


Figure 1. DEX induces muscle atrophy and pyroptosis in C2C12 myotubes. (A) Cell viability of C2C12 myotubes treated with different concentrations of DEX. n=5 per group. (B) Real-time PCR analysis of expression of muscle atrophic markers (Atrogin-1 and MuRF1) in C2C12 myotubes treated with 10 μ M DEX. n=6 per group. (C) Western blot analysis of expression level of Atrogin-1 and MuRF1 in C2C12 myotubes treated with 10 μ M DEX. GAPDH was used as a loading control. n=6 per group. (D) Western blot analysis of expression level of NLRP3, Caspase-1 and GSDMD in C2C12 myotubes treated with 10 μ M DEX. n=6 per group. * $P < 0.05$ vs. Ctrl, ** $P < 0.01$ vs. Ctrl. DEX, dexamethasone; Ctrl, control.

Knockdown of NLRP3/GSDMD alleviates dexamethasone-induced myotube pyroptosis and atrophy

Since NLRP3 inflammasome plays a crucial role in the activation of GSDMD dependent pyroptosis [14], we therefore investigated whether NLRP3/GSDMD pathway was involved in dexamethasone-induced myotube atrophy. We found that

dexamethasone-induced increase of Atrogin-1 and MuRF1 expression was alleviated by silencing GSDMD (Figure 2A and 2B). Moreover, dexamethasone-induced myotube atrophy was also attenuated by GSDMD inhibition, evidenced by increased C2C12 myotube diameter (21.06 ± 0.86 vs. $14.29 \pm 0.47\mu\text{m}$, $P < 0.01$, Figure 2C), indicating that pyroptosis may be one of the underlying mechanisms of glucocorticoid-induced muscle atrophy. In addition, knockdown of NLRP3 (Figure 2D) abolished the activation of Caspase-1-dependent pyroptosis as well as the increase of Atrogin-1 and MuRF1 induced by dexamethasone (Figure 2E). The decrease of C2C12 myotube diameter caused by dexamethasone treatment was also attenuated by NLRP3 inhibition (23.00 ± 0.95 vs. $13.68 \pm 0.59\mu\text{m}$, $P < 0.01$, Figure 2F). These results together demonstrate that knockdown of NLRP3/GSDMD pathway-mediated pyroptosis could ameliorate dexamethasone-induced myotube atrophy.

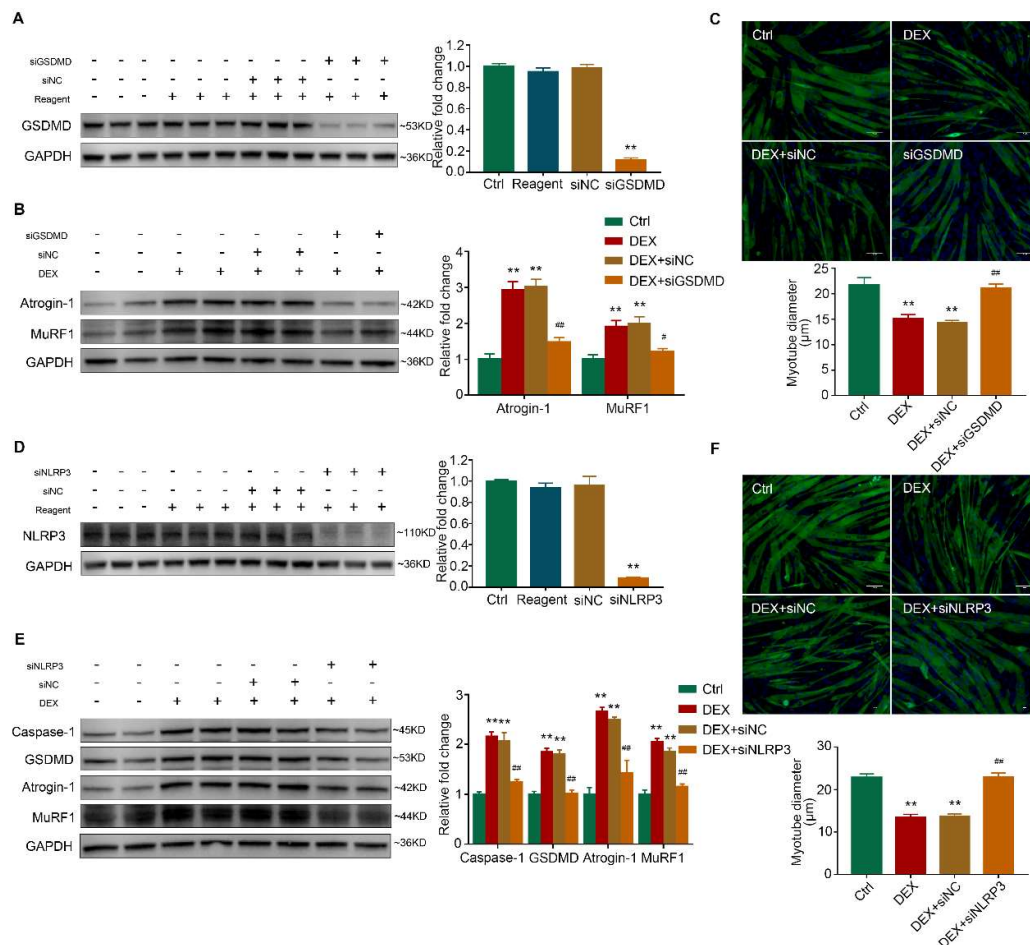


Figure 2. Inhibition of pyroptosis alleviates DEX-induced muscle atrophy in C2C12 myotubes. (A) C2C12 myotubes were transfected with negative control (siNC) or siRNA targeting GSDMD (siGSDMD). Protein levels of GSDMD were analyzed. $n=3$ per group. ** $P < 0.01$ vs. siNC. (B-C) C2C12 myotubes were treated with $10\mu\text{M}$ DEX combined with siNC or siGSDMD for 24 hours. Protein levels of Atrogin-1 and MuRF1 (B) and diameter of C2C12 myotubes (C) were analyzed. $n=4-5$ per group. ** $P < 0.01$ vs. Ctrl. # $P < 0.05$ vs. DEX+siNC, ## $P < 0.01$ vs. DEX+siNC. Scale bar = $50\mu\text{m}$. (D) C2C12 myotubes were transfected with negative control (siNC) or siRNA targeting NLRP3 (siNLRP3). Protein levels of NLRP3 were analyzed. $n=3$ per group. ** $P < 0.01$ vs. siNC. (E-F) C2C12 myotubes were treated with $10\mu\text{M}$ DEX combined with siNC or siNLRP3 for 24 hours. Protein levels of

Caspase-1, GSDMD, Atrogin-1 and MuRF1 (E) and diameter of C2C12 myotubes (F) were analyzed. $n=4-5$ per group. ** $P < 0.01$ vs. Ctrl. # $P < 0.05$ vs. DEX+siNC, ## $P < 0.01$ vs. DEX+siNC. Scale bar = 50 μ m. NC, normal control. DEX, dexamethasone.

Trimetazidine attenuates dexamethasone-induced C2C12 myotube atrophy

We further examined the effects of trimetazidine on myotube atrophy *in vitro*. Adding trimetazidine at concentrations of 50 μ M, 100 μ M, 150 μ M and 200 μ M to C2C12 myotubes did not reduce cell viability (Figure 3Aa). At the concentration of 150 μ M and 200 μ M, trimetazidine protected against dexamethasone-induced cell death (Figure 3Ab). Adding 150 μ M trimetazidine ameliorated dexamethasone-induced upregulation of Atrogin-1 and MuRF1 mRNA levels (Figure 3B). Similar results were observed in the protein levels of Atrogin-1 and MuRF1 (Figure 3C). Previous studies have suggested that the FoxO3a is involved in the activation of atrophy-linked ubiquitin ligases, including Atrogin-1 and MuRF1 [26, 27]. We found that the phosphorylation of FoxO3a was decreased by dexamethasone and was reversed by trimetazidine in C2C12 myotubes (Figure 3D). Moreover, dexamethasone-induced decreased C2C12 myotubes diameters were markedly reversed by trimetazidine (20.15 ± 0.69 vs. $12.60 \pm 0.89\mu$ m, $P < 0.01$, Figure 3E). The results indicate that trimetazidine can also attenuate dexamethasone-induced muscle atrophy *in vitro*.

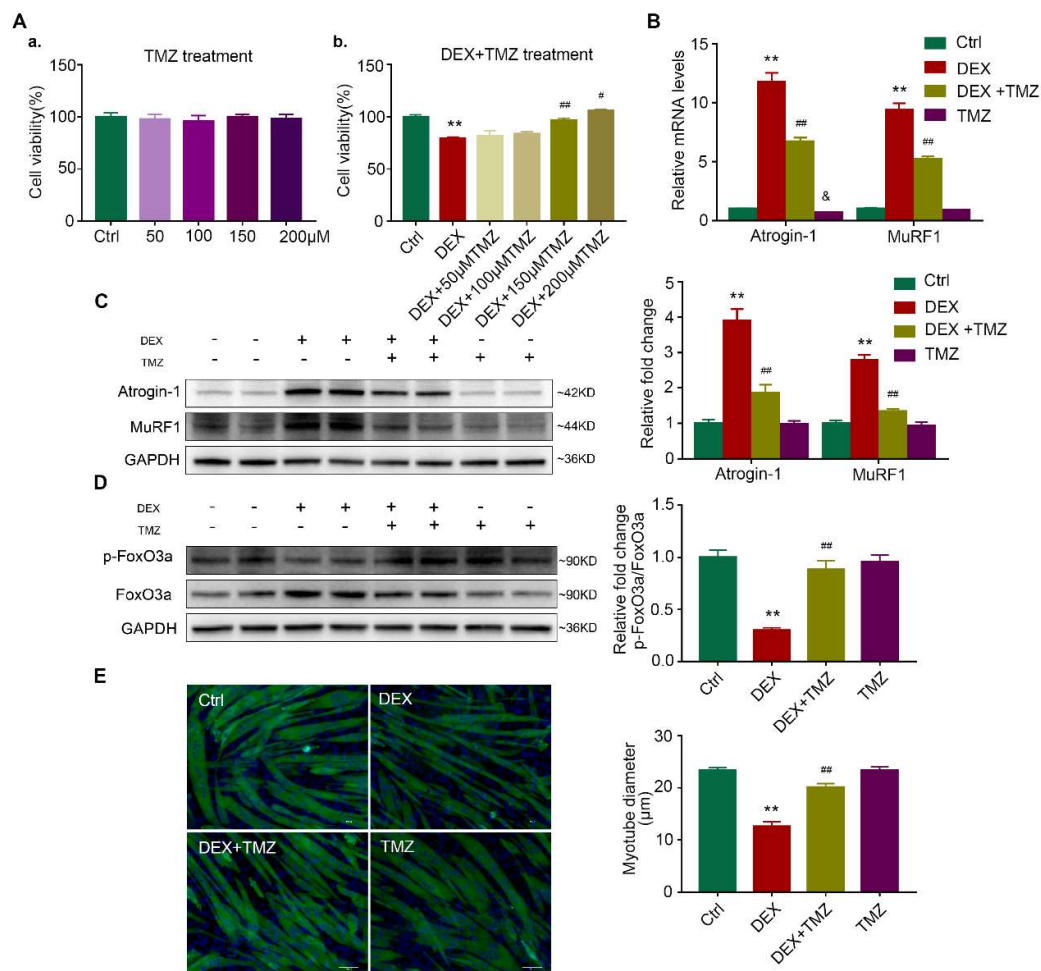


Figure 3. TMZ alleviates DEX-induced muscle atrophy in C2C12 myotubes. (A) Myotubes viability. a. C2C12 myotubes treated with different concentrations of TMZ. b.

C2C12 myotubes treated with DEX and TMZ. n=4-5 per group. (B) Real-time PCR analysis of expression of Atrogin-1 and MuRF1 in C2C12 myotubes treated with 10 μ M DEX and 150 μ M TMZ. n=4 per group. (C) Western blot analysis of expression levels of Atrogin-1 and MuRF1 in C2C12 myotubes treated with 10 μ M DEX and 150 μ M TMZ. n=6 per group. (D) Western blot analysis of expression level of p-FOXO3a and FOXO3a in C2C12 myotubes treated with 10 μ M DEX and 150 μ M TMZ. n=6 per group. (E) Diameter of C2C12 myotubes. n=5 per group. Scale bar = 50 μ m. ** $P < 0.01$ vs. Ctrl. # $P < 0.05$ vs. DEX. ## $P < 0.01$ vs. DEX. DEX, dexamethasone; TMZ, trimetazidine; Ctrl, control.

Trimetazidine alleviates dexamethasone-induced muscle atrophy in mice

To determine the protective effect of trimetazidine on muscle wasting, we established a model of dexamethasone-induced muscle atrophy in mice. The body weight was decreased in mice injected with dexamethasone when compared with control mice (Figure 4A). The results of running test indicated impaired exercise capacity in dexamethasone-treated mice, showing decreased running distance (181.94 ± 14.94 vs. 337.71 ± 41.98 m, Figure 4Ba) and running time (13.48 ± 0.94 vs. 21.03 ± 2.28 minutes, Figure 4Bb). Dexamethasone injection also induced significant muscle atrophy, especially in gastrocnemius and quadriceps (Figure 4C and Figure S2). Moreover, myofiber diameter was reduced by dexamethasone treatment (Figure 4D), together with elevated protein expression of Atrogin-1 and MuRF1 (Figure 4E). As expected, trimetazidine alleviated dexamethasone-induced loss of body weight (Figure 4A) and skeletal muscle weight in gastrocnemius (127.50 ± 5.26 vs. 105 ± 5.98 mg) and quadriceps (147.50 ± 6.48 vs. 121.25 ± 5.49 mg) (Figure 4C and Figure S2), as well as the decline of running distance (273.00 ± 16.88 vs. 181.94 ± 14.94 m, Figure 4Ba) and running time (16.84 ± 1.09 vs. 13.48 ± 0.94 minutes, Figure 4Bb). Moreover, dexamethasone-induced reduction of myofiber diameter (98.34 ± 5.46 vs. 77.61 ± 3.13 μ m, $P < 0.01$), upregulation of Atrogin-1 and MuRF1 (Figure 4E) and decreased phosphorylation of FoxO3a were also reversed by trimetazidine (Figure 4F). These data reveal that trimetazidine could attenuated dexamethasone-induced exercise intolerance and muscle atrophy.

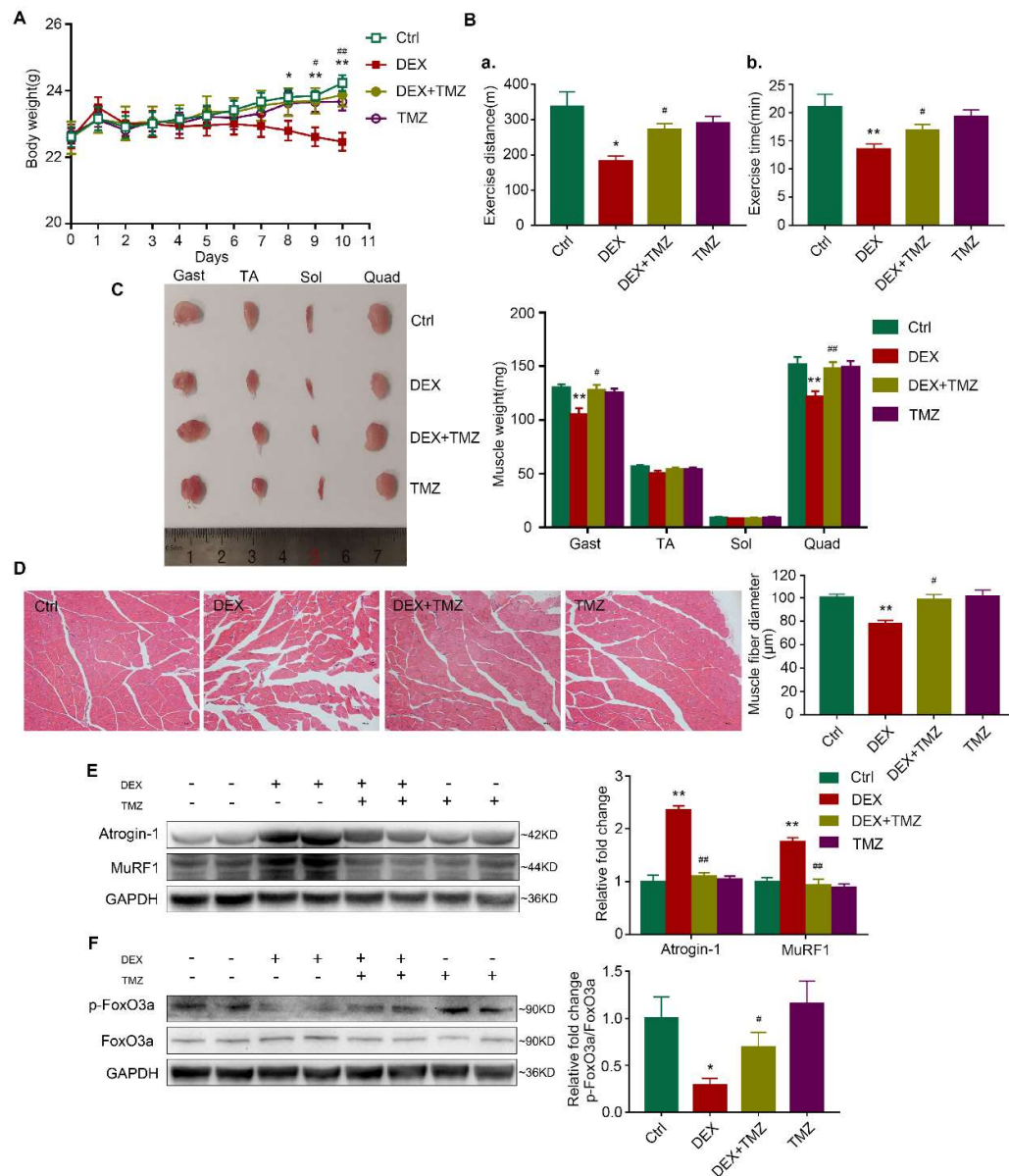


Figure 4. TMZ ameliorates DEX-induced muscle atrophy in mice. Mice were intraperitoneally inject with 0.9% saline (Ctrl), DEX (25 mg/kg), TMZ (5 mg/kg), or DEX (25 mg/kg)+TMZ (5 mg/kg). (A) Body weight of mice. n=8 per group. (B) Exercise capacity testing. a. Running distance. b. Running time. n=8 per group. (C) Comparison of representative samples of dissected skeletal muscle including gastrocnemius (Gast), tibialis anterior muscle (TA), soleus muscle (Sol), and quadriceps (Quad). n=4 per group. (D) Representative H&E staining of myofiber cross section of Gast. Scale bar = 100 μ m. A microscope with a 40 \times objective was used to capture the images. n=5 per group. (E) Western blot analysis of expression levels of Atrogin-1 and MuRF1 in Gast muscle. n=6 per group. (F) Western blot analysis of expression levels of p-FOXO3a and FOXO3a in Gast muscle. n=6 per group. * $P < 0.05$ vs. Ctrl. ** $P < 0.01$ vs. Ctrl. # $P < 0.05$ vs. DEX. ## $P < 0.01$ vs. DEX. DEX, dexamethasone; TMZ, trimetazidine; Ctrl, control.

Trimetazidine mitigates dexamethasone-induced pyroptosis *in vitro* and *in vivo*

Pyroptosis plays an important role in the development of muscle atrophy [15], and trimetazidine has been shown to have the ability of inhibiting pyroptosis [22]. Treating

C2C12 myotubes with dexamethasone increased the mRNA expression of pyroptosis-related molecules, including NLRP3, Caspase-1, GSDMD, Caspase-4 and IL-1 β (Figure 5A). Consistently, the protein levels of NLRP3, Caspase-1, GSDMD were also elevated in dexamethasone-treated C2C12 myotubes (Figure 5B). Importantly, the upregulated pyroptosis-related genes induced by dexamethasone were mitigated by trimetazidine (Figure 5A and 5B). Similar to the results in C2C12 myotubes, trimetazidine also markedly attenuated dexamethasone-induced increase of NLRP3, GSDMD, Caspase-1, IL-1 β and IL-18 expressions (Figure 5C) in mice. These results indicate that trimetazidine can protect against dexamethasone-induced pyroptosis in skeletal muscle.

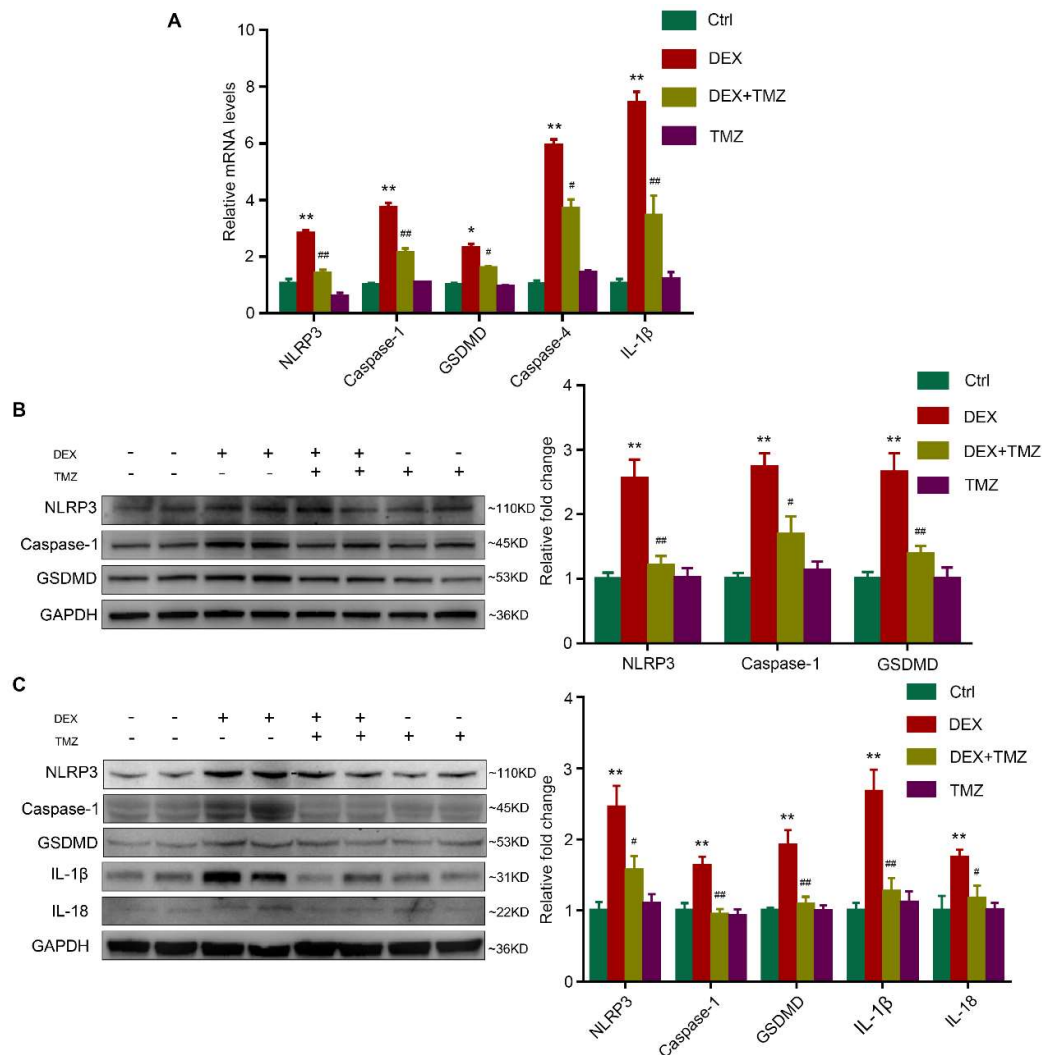


Figure 5. TMZ attenuates DEX-induced pyroptosis in myotubes and mice. (A-B) C2C12 myotubes treated with 10 μ M DEX combined with or without 150 μ M TMZ. mRNA levels of NLRP3, Caspase-1, GSDMD, Caspase-4 and IL-1 β (A) protein levels of NLRP3, Caspase-1, GSDMD (B) were analyzed. n=4-6 per group. (C) Mice were intraperitoneally inject with 0.9% saline (Ctrl), DEX (25 mg/kg), TMZ (5 mg/kg), or DEX (25 mg/kg)+TMZ (5 mg/kg). Protein levels of NLRP3, Caspase-1, GSDMD, IL-1 β and IL-18 were analyzed in gastrocnemius. n=6 per group. * $P < 0.05$ vs. Ctrl. ** $P < 0.01$ vs. Ctrl. # $P < 0.05$ vs. DEX. ## $P < 0.01$ vs. DEX. DEX, dexamethasone; TMZ, trimetazidine; Ctrl, control.

Discussion

Skeletal muscle atrophy is one of the major side effects of high dose or the sustained usage of glucocorticoids [11]. Pyroptosis is involved in the development of muscle atrophy [15]. We here show that dexamethasone treatment induces muscle atrophy and pyroptosis both *in vitro* and *in vivo*. Inhibiting pyroptosis by knockdown NLRP3/GSDMD pathway alleviates dexamethasone-induced myotube atrophy. Trimetazidine exerts protective effects on improving dexamethasone-induced exercise intolerance *in vivo*, as evidenced by increased running distance and running time. Such a protection relies on the suppression of pyroptosis induced by dexamethasone, since trimetazidine treatment reverse dexamethasone-induced activation of pyroptosis both in C2C12 cells and in mice. Therefore, trimetazidine may be a promising therapeutic agent for the prevention of glucocorticoids-induced skeletal muscle atrophy.

Skeletal muscle comprises approximately 40% of body mass and is a major target of glucocorticoids [10, 28]. Plenty of evidence indicates that glucocorticoids can cause muscle atrophy which is accompanied by decreased protein synthesis and increased degradation in muscles; in particular, the ubiquitin-proteasome system is most prominent mechanism of protein breakdown [10, 29]. In the ubiquitin proteasome pathway, FoxO3a is considered as a key player in the control of skeletal muscle protein turnover [30]. The activation of FoxO3a caused by dephosphorylation induces nuclear translocation, which in turn enhances the expression of two E3 ubiquitin ligases, MuRF1 and Atrogin-1 [31, 32]. As expected, our data showed that the phosphorylated level of FoxO3a was decreased by dexamethasone treatment, resulting in elevated expression of Atrogin-1 and MuRF1. Interestingly, dexamethasone-induced muscle atrophy was remarkably reversed by trimetazidine which is a well-known anti-anginal agent (Figure 3 and 4). Our results are consistent with previous studies showing that trimetazidine exerts anti-atrophy effects in skeletal muscle either via inducing autophagy [20] or enhancing mitochondrial quality control [33]. Indeed, the improvement of trimetazidine treatment on physical performance and muscle endurance has been demonstrated in patients with ischemic heart disease [34, 35]. Further clinical studies are needed to assess the efficacy and safety of trimetazidine treatment in patients with muscle dysfunction or sarcopenia.

Inflammation has been identified as the major mechanism for muscle atrophy under various stimuli [36]. Pyroptosis is a novel pro-inflammatory programmed cell death that produces IL-1 β and IL-18 which in turn impair skeletal muscle function [37]. Recently, Ding *et al.* [15] showed that Pyroptosis was activated in the gastrocnemius of cigarette smoke exposure-induced muscle atrophy mice model. Our present study demonstrated that dexamethasone treatment increased the expression of pyroptosis-related genes, including GSDMD, IL-1 β and IL-18 both in C2C12 myotubes (Figure 1C) and in mice (Figure 5). Inhibition of pyroptosis by silencing GSDMD significantly alleviated dexamethasone-induced upregulation of MuRF1 and Atrogin-1 (Figure 2B). Although glucocorticoids are commonly used as anti-inflammatory agents, our results provide new insights into mechanisms of how sustained or high-dose use of glucocorticoids cause muscle pyroptosis and atrophy.

The activation of NLRP3 inflammasome may be an important mechanism for glucocorticoids-induced myocyte pyroptosis. The NLRP3 inflammasome cleaves pro-inflammatory IL-1 β and IL-18 [14]. Emerging literature shows that NLRP3 inflammasome is activated in skeletal muscle in multiple muscle atrophy models [37-40]. NLRP3 inflammasome responds to various stimuli including infection, reactive oxygen species, metabolic stress, and even therapeutic drugs such as statins [41, 42]. Recent studies indicate that glucocorticoids can also modulate the assembly

of the NLRP3 inflammasome [43, 44]. Consistently, dexamethasone treatment increased the expression of NLRP3 and Caspase-1 in C2C12 myotubes (Figure 1C) and mice (Figure 5). Knockdown of NLRP3 attenuated dexamethasone-induced muscle pyroptosis and atrophy (Figure 2D and 2E), indicating that dexamethasone triggers myocyte pyroptosis via activating NLRP3 inflammasome. Taken together, these data suggest that NLRP3 may potentially be a therapeutic target for the treatment of skeletal muscle atrophy.

Another interesting finding of our study is that dexamethasone-induced pyroptosis was also attenuated by trimetazidine treatment. Trimetazidine is a partial fatty acid oxidation inhibitor due to the suppression of long-chain 3 ketoacyl coenzyme A thiolase activity [45]. Recent studies have shown that trimetazidine possesses anti-inflammatory properties and plays cytoprotective roles in various tissues, including heart, brain, and renal tissue [46-48]. In septic cardiac dysfunction model, trimetazidine attenuated lipopolysaccharide-induced cardiomyocyte pyroptosis by promoting neutrophils recruitment to the heart tissue [22]. We now provide one mechanistic explanation for the therapeutic potential of trimetazidine in glucocorticoids-induced muscle atrophy in that it inhibits pyroptosis. Consistent with this, trimetazidine treatment decreases dexamethasone-induced upregulation of NLRP3, Caspase-1, GSDMD, IL-1 β and IL-18 in skeletal muscle (Figure 5).

Conclusions

In summary, our data reveal a novel mechanism of dexamethasone-induced skeletal muscle atrophy. Dexamethasone induces muscle atrophy not just through activating FoxO3a by dephosphorylation, but also via inducing NLRP3/GSDMD pathway-mediated pyroptosis in skeletal muscle. Trimetazidine may alleviate dexamethasone-induced skeletal muscle atrophy partially via inhibiting pyroptosis (Figure 6). Therefore, trimetazidine might be a potential therapeutic compound for the prevention of muscle atrophy in glucocorticoid-treated patients.

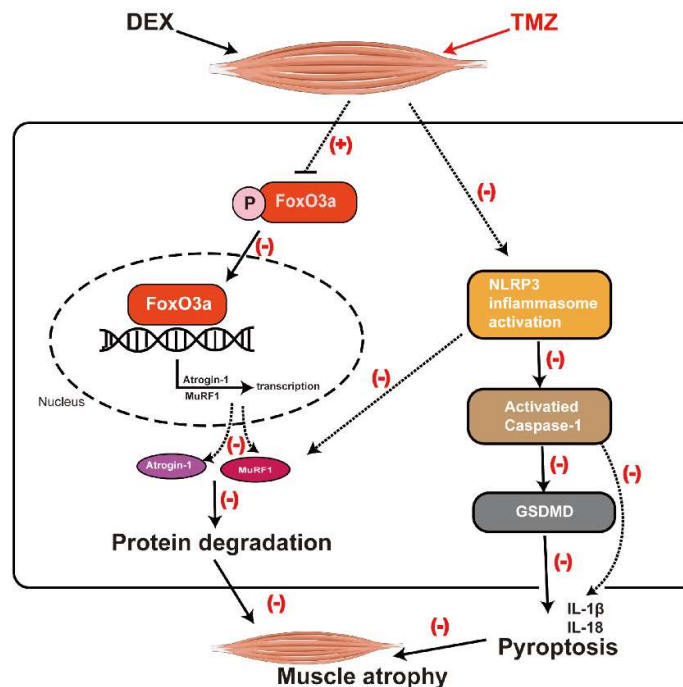


Figure 6. Schematic of the mechanism by which TMZ attenuates DEX-induced skeletal

muscle atrophy via inhibiting pyroptosis. DEX induces muscle atrophy not just through activating FoxO3a by dephosphorylation, but also via inducing NLRP3/GSDMD pathway-mediated pyroptosis in skeletal muscle, which can be alleviated by TMZ. Black arrows represent the role of DEX, red plus (+) and minus signs (-) represent the role of TMZ. DEX, dexamethasone. TMZ, trimetazidine.

Author contributions

Wei Gao and Xiang Lu designed the research, interpreted the data, and contributed to revising the manuscript. Li Wang and Ming-Qing He performed the research, analyzed the data, and wrote the manuscript. Xi-Yu Shen, Kang-Zhen Zhang, Can Zhao, Li Liu and Hui-Wei He analyzed data and contributed to discussion.

Funding Statement

This work was supported by grants from the National Natural Science Foundation of China (No. 81770440 and 81970218 to Xiang Lu and No. 81700331 and 81970217 to Wei Gao, No.81901262 to Ming-Qing He), a grant from the Natural Science Foundation of Jiangsu Province (No. BK20171051 to Wei Gao and No. BK20190171 to Ming-Qing He), the Jiangsu Province Health Development Project with Science and Education (No. QNRC201685 to Wei Gao), a grant from the Six One Project of Jiangsu Province (No. LGY2018100 to Wei Gao), a grant from the Six Talent Peaks Project of Jiangsu Province (No. WSN- 175 to Wei Gao), a grant from Science and Technology Project for the Youth of Suzhou (No. KJXW2018009 to Ming-Qing He), and grants from the Postgraduate Research & Practice Innovation Program of Jiangsu Province (No. SJCX18_0427 to Li Wang and No. KYCX19_1183 to Xi-Yu Shen).

Data Availability

All data and materials used for this study are displayed or can be displayed upon request.

Conflict of Interest statement

The authors declare no conflict of interest.

References

1. Larsson, L.; Degens, H.; Li, M.; Salvati, L.; Lee, Y. I.; Thompson, W.; Kirkland, J. L.; Sandri, M., Sarcopenia: Aging-Related Loss of Muscle Mass and Function. *Physiological reviews* **2019**, 99, (1), 427-511.
2. Cohen, S.; Nathan, J. A.; Goldberg, A. L., Muscle wasting in disease: molecular mechanisms and promising therapies. *Nature reviews. Drug discovery* **2015**, 14, (1), 58-74.
3. Naseeb, M. A.; Volpe, S. L., Protein and exercise in the prevention of sarcopenia and aging. *Nutr Res* **2017**, 40, 1-20.
4. Zhang, X.; Edwards, B. J., Malnutrition in Older Adults with Cancer. *Current oncology reports* **2019**, 21, (9), 80.
5. Cruz-Jentoft, A. J.; Kiesswetter, E.; Drey, M.; Sieber, C. C., Nutrition, frailty, and sarcopenia. *Aging clinical and experimental research* **2017**, 29, (1), 43-48.
6. Yin, J.; Lu, X.; Qian, Z.; Xu, W.; Zhou, X., New insights into the pathogenesis and treatment of sarcopenia in chronic heart failure. *Theranostics* **2019**, 9, (14), 4019-4029.
7. Kalinkovich, A.; Livshits, G., Sarcopenic obesity or obese sarcopenia: A cross talk between age-associated adipose tissue and skeletal muscle inflammation as a main mechanism of the pathogenesis. *Ageing research reviews* **2017**, 35, 200-221.
8. Landi, F.; Calvani, R.; Cesari, M.; Tosato, M.; Martone, A. M.; Ortolani, E.; Saveria,

- G.; Salini, S.; Sisto, A.; Picca, A.; Marzetti, E., Sarcopenia: An Overview on Current Definitions, Diagnosis and Treatment. *Current protein & peptide science* **2018**, 19, (7), 633-638.
9. Williams, S.; Ghosh, C., Neurovascular glucocorticoid receptors and glucocorticoids: implications in health, neurological disorders and drug therapy. *Drug discovery today* **2020**, 25, (1), 89-106.
10. Bodine, S. C.; Furlow, J. D., Glucocorticoids and Skeletal Muscle. *Advances in experimental medicine and biology* **2015**, 872, 145-76.
11. Schakman, O.; Kalista, S.; Barbe, C.; Loumaye, A.; Thissen, J. P., Glucocorticoid-induced skeletal muscle atrophy. *The international journal of biochemistry & cell biology* **2013**, 45, (10), 2163-72.
12. Fappi, A.; Neves, J. C.; Sanches, L. N.; Massaroto, E. S. P. V.; Sikusawa, G. Y.; Brandao, T. P. C.; Chadi, G.; Zanoteli, E., Skeletal Muscle Response to Deflazacort, Dexamethasone and Methylprednisolone. *Cells* **2019**, 8, (5).
13. Kroemer, G.; Galluzzi, L.; Vandenabeele, P.; Abrams, J.; Alnemri, E. S.; Baehrecke, E. H.; Blagosklonny, M. V.; El-Deiry, W. S.; Golstein, P.; Green, D. R.; Hengartner, M.; Knight, R. A.; Kumar, S.; Lipton, S. A.; Malorni, W.; Nunez, G.; Peter, M. E.; Tschoop, J.; Yuan, J.; Piacentini, M.; Zhivotovsky, B.; Melino, G., Classification of cell death: recommendations of the Nomenclature Committee on Cell Death 2009. *Cell death and differentiation* **2009**, 16, (1), 3-11.
14. Xue, Y.; Enosi Tuipulotu, D.; Tan, W. H.; Kay, C.; Man, S. M., Emerging Activators and Regulators of Inflammasomes and Pyroptosis. *Trends in immunology* **2019**, 40, (11), 1035-1052.
15. Ding, J.; Li, F.; Cong, Y.; Miao, J.; Wu, D.; Liu, B.; Wang, L., Trichostatin A inhibits skeletal muscle atrophy induced by cigarette smoke exposure in mice. *Life sciences* **2019**, 235, 116800.
16. Heggermont, W. A.; Papageorgiou, A. P.; Heymans, S.; van Bilsen, M., Metabolic support for the heart: complementary therapy for heart failure? *European journal of heart failure* **2016**, 18, (12), 1420-1429.
17. Belardinelli, R.; Lacalaprice, F.; Faccenda, E.; Volpe, L., Trimetazidine potentiates the effects of exercise training in patients with ischemic cardiomyopathy referred for cardiac rehabilitation. *European journal of cardiovascular prevention and rehabilitation : official journal of the European Society of Cardiology, Working Groups on Epidemiology & Prevention and Cardiac Rehabilitation and Exercise Physiology* **2008**, 15, (5), 533-40.
18. Ferraro, E.; Pin, F.; Gorini, S.; Pontecorvo, L.; Ferri, A.; Mollace, V.; Costelli, P.; Rosano, G., Improvement of skeletal muscle performance in ageing by the metabolic modulator Trimetazidine. *Journal of cachexia, sarcopenia and muscle* **2016**, 7, (4), 449-57.
19. Molinari, F.; Pin, F.; Gorini, S.; Chiandotto, S.; Pontecorvo, L.; Penna, F.; Rizzuto, E.; Pisu, S.; Musaro, A.; Costelli, P.; Rosano, G.; Ferraro, E., The mitochondrial metabolic reprogramming agent trimetazidine as an 'exercise mimetic' in cachectic C26-bearing mice. *Journal of cachexia, sarcopenia and muscle* **2017**, 8, (6), 954-973.
20. Ferraro, E.; Giammarioli, A. M.; Caldarola, S.; Lista, P.; Feraco, A.; Tinari, A.; Salvatore, A. M.; Malorni, W.; Berghella, L.; Rosano, G., The metabolic modulator trimetazidine triggers autophagy and counteracts stress-induced atrophy in skeletal muscle myotubes. *The FEBS journal* **2013**, 280, (20), 5094-108.
21. Song, M.; Chen, F. F.; Li, Y. H.; Zhang, L.; Wang, F.; Qin, R. R.; Wang, Z. H.; Zhong, M.; Tang, M. X.; Zhang, W.; Han, L., Trimetazidine restores the positive adaptation to exercise training by mitigating statin-induced skeletal muscle injury. *Journal of cachexia, sarcopenia and muscle* **2018**, 9, (1), 106-118.
22. Chen, J.; Wang, B.; Lai, J.; Braunstein, Z.; He, M.; Ruan, G.; Yin, Z.; Wang, J.; Cianflone, K.; Ning, Q.; Chen, C.; Wang, D. W., Trimetazidine Attenuates Cardiac Dysfunction in Endotoxemia and Sepsis by Promoting Neutrophil Migration. *Frontiers in immunology* **2018**, 9, 2015.

23. Mille-Hamard, L.; Billat, V. L.; Henry, E.; Bonnamy, B.; Joly, F.; Benech, P.; Barrey, E., Skeletal muscle alterations and exercise performance decrease in erythropoietin-deficient mice: a comparative study. *BMC medical genomics* **2012**, 5, 29.
24. Rommel, C.; Bodine, S. C.; Clarke, B. A.; Rossman, R.; Nunez, L.; Stitt, T. N.; Yancopoulos, G. D.; Glass, D. J., Mediation of IGF-1-induced skeletal myotube hypertrophy by PI(3)K/Akt/mTOR and PI(3)K/Akt/GSK3 pathways. *Nature cell biology* **2001**, 3, (11), 1009-13.
25. Chiu, H. C.; Chiu, C. Y.; Yang, R. S.; Chan, D. C.; Liu, S. H.; Chiang, C. K., Preventing muscle wasting by osteoporosis drug alendronate in vitro and in myopathy models via sirtuin-3 down-regulation. *Journal of cachexia, sarcopenia and muscle* **2018**, 9, (3), 585-602.
26. Guo, Y.; Wang, H.; Tang, Y.; Wang, Y.; Zhang, M.; Yang, Z.; Nyirimigabo, E.; Wei, B.; Lu, Z.; Ji, G., GCN2 deficiency protects mice from denervation-induced skeletal muscle atrophy via inhibiting FoxO3a nuclear translocation. *Protein & cell* **2018**, 9, (11), 966-970.
27. Luo, J.; Liang, A.; Liang, M.; Xia, R.; Rizvi, Y.; Wang, Y.; Cheng, J., Serum Glucocorticoid-Regulated Kinase 1 Blocks CKD-Induced Muscle Wasting Via Inactivation of FoxO3a and Smad2/3. *Journal of the American Society of Nephrology : JASN* **2016**, 27, (9), 2797-808.
28. Frontera, W. R.; Ochala, J., Skeletal muscle: a brief review of structure and function. *Calcified tissue international* **2015**, 96, (3), 183-95.
29. Pereira, R. M.; Freire de Carvalho, J., Glucocorticoid-induced myopathy. *Joint, bone, spine : revue du rhumatisme* **2011**, 78, (1), 41-4.
30. Goodman, C. A., The role of mTORC1 in regulating protein synthesis and skeletal muscle mass in response to various mechanical stimuli. *Reviews of physiology, biochemistry and pharmacology* **2014**, 166, 43-95.
31. Sandri, M.; Sandri, C.; Gilbert, A.; Skurk, C.; Calabria, E.; Picard, A.; Walsh, K.; Schiaffino, S.; Lecker, S. H.; Goldberg, A. L., Foxo transcription factors induce the atrophy-related ubiquitin ligase atrogin-1 and cause skeletal muscle atrophy. *Cell* **2004**, 117, (3), 399-412.
32. Shen, S.; Liao, Q.; Liu, J.; Pan, R.; Lee, S. M.; Lin, L., Myricanol rescues dexamethasone-induced muscle dysfunction via a sirtuin 1-dependent mechanism. *Journal of cachexia, sarcopenia and muscle* **2019**, 10, (2), 429-444.
33. Xie, M.; Jiang, L.; Dun, Y.; Zhang, W.; Liu, S., Trimetazidine combined with exercise improves exercise capacity and anti-fatal stress ability through enhancing mitochondrial quality control. *Life sciences* **2019**, 224, 157-168.
34. Vitale, C.; Marazzi, G.; Pelliccia, F.; Volterrani, M.; Cerquetani, E.; Spoletini, I.; Mercuro, G.; Bonassi, S.; Dall'Armi, V.; Fini, M.; Rosano, G. M., Trimetazidine improves exercise performance in patients with peripheral arterial disease. *Pharmacological research* **2011**, 63, (4), 278-83.
35. Zhao, Y.; Peng, L.; Luo, Y.; Li, S.; Zheng, Z.; Dong, R.; Zhu, J.; Liu, J., Trimetazidine improves exercise tolerance in patients with ischemic heart disease : A meta-analysis. *Herz* **2016**, 41, (6), 514-22.
36. Chhetri, J. K.; de Souto Barreto, P.; Fougere, B.; Rolland, Y.; Vellas, B.; Cesari, M., Chronic inflammation and sarcopenia: A regenerative cell therapy perspective. *Experimental gerontology* **2018**, 103, 115-123.
37. Gugliandolo, A.; Giacoppo, S.; Bramanti, P.; Mazzon, E., NLRP3 Inflammasome Activation in a Transgenic Amyotrophic Lateral Sclerosis Model. *Inflammation* **2018**, 41, (1), 93-103.
38. Huang, N.; Kny, M.; Riediger, F.; Busch, K.; Schmidt, S.; Luft, F. C.; Slevogt, H.; Fielitz, J., Deletion of Nlrp3 protects from inflammation-induced skeletal muscle atrophy. *Intensive care medicine experimental* **2017**, 5, (1), 3.
39. McBride, M. J.; Foley, K. P.; D'Souza, D. M.; Li, Y. E.; Lau, T. C.; Hawke, T. J.; Schertzer, J. D., The NLRP3 inflammasome contributes to sarcopenia and lower

- muscle glycolytic potential in old mice. *American journal of physiology. Endocrinology and metabolism* **2017**, 313, (2), E222-E232.
40. Liu, Y.; Bi, X.; Zhang, Y.; Wang, Y.; Ding, W., Mitochondrial dysfunction/NLRP3 inflammasome axis contributes to angiotensin II-induced skeletal muscle wasting via PPAR-gamma. *Laboratory investigation; a journal of technical methods and pathology* **2020**, 100, (5), 712-726.
 41. Kelley, N.; Jeltema, D.; Duan, Y.; He, Y., The NLRP3 Inflammasome: An Overview of Mechanisms of Activation and Regulation. *International journal of molecular sciences* **2019**, 20, (13).
 42. Henriksbo, B. D.; Lau, T. C.; Cavallari, J. F.; Denou, E.; Chi, W.; Lally, J. S.; Crane, J. D.; Duggan, B. M.; Foley, K. P.; Fullerton, M. D.; Tarnopolsky, M. A.; Steinberg, G. R.; Schertzer, J. D., Fluvastatin causes NLRP3 inflammasome-mediated adipose insulin resistance. *Diabetes* **2014**, 63, (11), 3742-7.
 43. Busillo, J. M.; Azzam, K. M.; Cidlowski, J. A., Glucocorticoids sensitize the innate immune system through regulation of the NLRP3 inflammasome. *The Journal of biological chemistry* **2011**, 286, (44), 38703-13.
 44. Frank, M. G.; Hershman, S. A.; Weber, M. D.; Watkins, L. R.; Maier, S. F., Chronic exposure to exogenous glucocorticoids primes microglia to pro-inflammatory stimuli and induces NLRP3 mRNA in the hippocampus. *Psychoneuroendocrinology* **2014**, 40, 191-200.
 45. Folmes, C. D.; Clanachan, A. S.; Lopaschuk, G. D., Fatty acid oxidation inhibitors in the management of chronic complications of atherosclerosis. *Current atherosclerosis reports* **2005**, 7, (1), 63-70.
 46. Tang, S. G.; Liu, X. Y.; Wang, S. P.; Wang, H. H.; Jovanovic, A.; Tan, W., Trimetazidine prevents diabetic cardiomyopathy by inhibiting Nox2/TRPC3-induced oxidative stress. *Journal of pharmacological sciences* **2019**, 139, (4), 311-318.
 47. Wan, P.; Su, W.; Zhang, Y.; Li, Z.; Deng, C.; Zhuo, Y., Trimetazidine protects retinal ganglion cells from acute glaucoma via the Nrf2/Ho-1 pathway. *Clin Sci (Lond)* **2017**, 131, (18), 2363-2375.
 48. Gelosa, P.; Banfi, C.; Brioschi, M.; Nobili, E.; Gianella, A.; Guerrini, U.; Pignieri, A.; Tremoli, E.; Sironi, L., S 35171 exerts protective effects in spontaneously hypertensive stroke-prone rats by preserving mitochondrial function. *European journal of pharmacology* **2009**, 604, (1-3), 117-24.